Sensitivity numerical simulations of Hurricane Patricia (2015) on lateral boundary conditions and inhibition rate of evaporation

Akiyoshi Wada
Meteorological Research Institute, Tsukuba, Ibaraki, 305-0052, JAPAN
awada@mri-jma.go.jp

1. Introduction

Hurricane Patricia (2015) was a historic tropical cyclone (TC) that broke historical records such as intensification rate during the intensification phase, maximum intensity during the mature phase and weakening rate during the decaying phase in late October 2015 in the eastern North Pacific (Rogers et al., 2017). Rogers et al (2017) pointed out that the storm was extremely small so that it could not be well-depicted using a numerical model grid with a grid spacing of 2-3 km. In addition, the simulation of the storm could be affected by experimental design such as the width of a sponge layer for lateral boundary condition, which is necessary for a regional atmosphere model, and values of parameters associated with cloud physics. Thus, we performed sensitivity numerical simulations of Patricia to the width of the sponge layer for lateral boundary condition and inhibition rate of evaporation of rain, snow and graupel by using a nonhydrostatic atmosphere model (NHM) with a grid spacing of 1 km.

2. Data and method

Figure 1 shows the computational domain. It covered a 1080 km x 1080 km area with a horizontal grid spacing of 1 km. The integration time was 48 hours and the initial time was 0600 UTC on 22 October in 2015. NHM had 55 vertical levels with variable intervals from 40 m for the near-surface layer to 1013 m for the uppermost layer. The top height was ~26 km. The simulations used the Japan Meteorological Agency global objective analysis data (with a horizontal grid spacing of ~20km) for creating atmospheric initial and boundary conditions and the daily oceanic reanalysis data calculated by the Meteorological Research Institute multivariate ocean variational estimation (MOVE) system (Usui, et al. 2006) with a horizontal grid spacing of 0.5˚.

For sensitivity numerical experiments, the width of the sponge layer (IDIFX) was set to 10, 40 and 70, respectively (see Table 1). The inhibition rate of evaporation of rain, snow and graupel was set to 0.0, 0.5 and 1.0, respectively. The control run (CNTL) was defined with IDIFX=10 and the value of the inhibition rate=0.0.

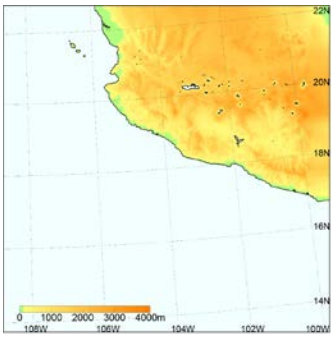

Figure 1 Computational domain. Colors indicate land elevation.

Table 1 Control and sensitivity experiments

Experiment	IDIFX	Inhibition rate (rain, snow, graupel)
CNTL (X10,E0.0)	10	0.0
X40	40	0.0
X70	70	0.0
E0.5	10	0.5
E1.0	10	1.0

3. Results

3.1 Track and central-pressure simulation

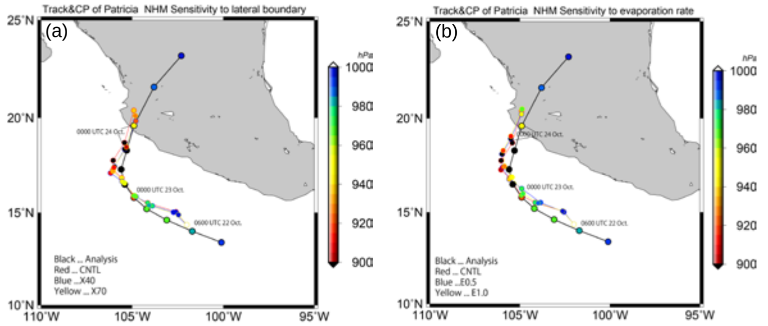

Figure 2 Results of track simulations of Patricia for (a) sensitivity to lateral boundary conditions and (b) inhibition rate of evaporation.

Figure 2 shows the results of track simulations. The width of the sponge layer (Figure 2a) and the value of inhibition rate (Figure 2b) were not sensitive to the simulated tracks. All simulated tracks had a northward bias at an earlier integration time, and then they had a westward bias after the recurvature. Less sensitivity of track simulations to these parameters indicates that these biases and slow translation were caused by atmospheric initial conditions used in the simulations.

Figure 3 shows the results of the simulations of central pressure and maximum surface wind speed. All simulations poorly depicted the early rapid intensification and peak intensity at 1200 UTC on 23 October. However, the simulations well depicted the weakening rate during the decaying phase although the timing was late due to slow translation of simulated storm.

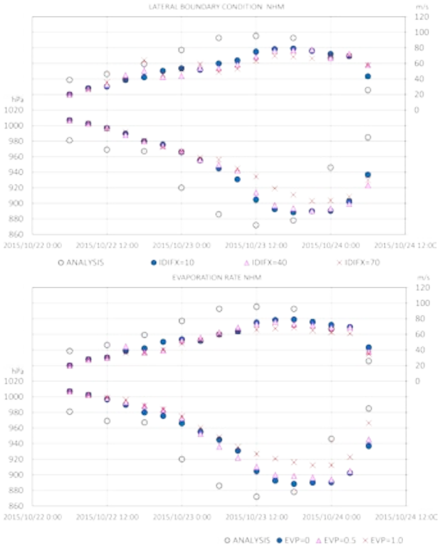

Figure 3 Results of the simulations of central pressure and maximum surface wind speed for (a) sensitivity to lateral boundary conditions and (b) inhibition rate of evaporation.

3.2 Sensitivity of the inner-core structure to lateral boundary conditions and evaporation rate

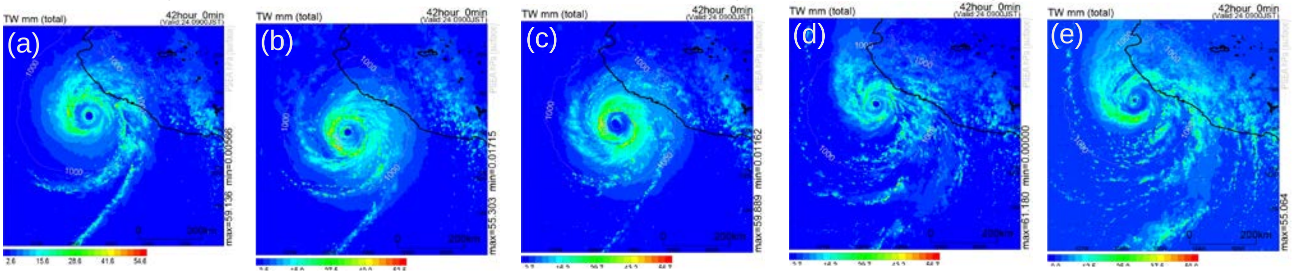

Figure 4 Horizontal distributions of total water content (shades) in a grid column from the surface to the 44th level in (a) CNTL, (b) X40, (c) X70, (d) E0.5 and (e) E1.0 experiments at 42h (corresponding to 0000 UTC 24 October). Contour intervals are 40 hPa.

Figure 4 shows the horizontal distributions of total water content in each experiment at the 42-hour integration time (42h), corresponding to 0000 UTC 24 October. The distributions quite differed among the five experiments. Some experiments depicted a distinct double eyewall structure (Figs. 4a, 4d and 4e), which is consistent with AMSR-2 89GHz brightness temperature image (Fig.11 in Rogers et al., 2017). A relatively large width of the sponge layer inhibited the formation of the inner distinct eyewall structure. A larger number of the inhabitation rate of evaporation of rain, snow and graupel did affect a smaller size of the inner distinct eyewall structure although the storm intensity in the CNTL experiment was stronger than that in the E1.0 experiment. The smaller size of the inner distinct eyewall structure is consistent with AMSR-2 89GHz brightness temperature image (Fig.11 in Rogers et al., 2017). The results suggest that experimental design of numerical simulation for TCs is important to depict the intensity and the inner core structure. It should be noted that spiral rainbands outside the inner core of the TC became remarkable in the E0.5 and E1.0 experiments, while the intensity was relatively weak.

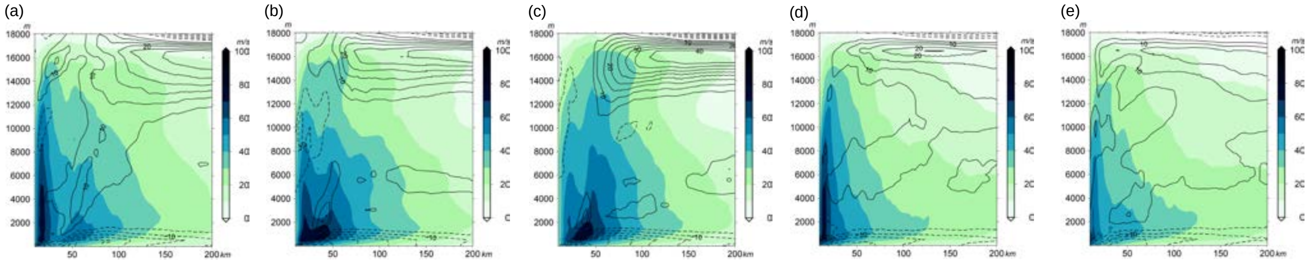

Figure 5 Axisymmetric mean vertical profiles of tangential winds (shades: m/s) and radial winds (contours: m/s) in (a) CNTL, (b) X40, (c) X70, (d) E0.5 and (e) E1.0 experiments at 42h (corresponding to 0000 UTC 24 October). Solid contours indicate outflow, while dashed contours indicate inflow (to the TC center). Contour intervals are 5 m/s.

Figure 5 shows axisymmetric mean vertical profiles of radial and tangential flows in each experiment at 42h. The CNTL experiment depicted a distinct double eyewall structure, which is consistent with the result of composite analysis in Rogers et al. (2017). The inner eyewall became weaker as the width of the sponge layer increased. The location of the outer eyewall changed inward so that the outer eyewall was dominant in the X70 experiment. This suggests that the atmospheric environment could affect the eyewall replacement process. The outer eyewall was not well simulated in the E0.5 and E1.0 experiments. In the E1.0 experiment, both primary and secondary circulations became weak. The result indicates that the inhibition of evaporation of rain, snow and graupel played a crucial role in weakening the TC.

4. Concluding remarks

Hurricane Patricia was a historic tropical cyclone in view of the intensification rate, maximum intensity and weakening rate during the decaying phase and its storm size was extremely small. NHM with a grid spacing of 1 km was used for investigating the sensitivity of numerical simulations to the width of the sponge layer and inhibition rate of evaporation of rain, snow and graupel. These two factors did affect the intensity simulations and the inner-core structure. This study did not consider the effect of ocean coupling because of slow translation of simulated storm and resultant excessive TC-induced sea surface cooling simulated by a coupled atmosphere-wave-ocean model (Wada et al., 2010). To reduce the bias of the simulation of Patricia, oceanic initial conditions should be improved in addition to understanding of the role of physical processes and atmospheric boundary conditions in TC simulations.

Acknowledgements

This work was supported by JSPS KAKENHI Grant Number JP15K05292.

References

Rogers R. F., S. Aberson, M. M. Bell, D. J. Cecil, J. D. Doyle, T. B. Kimberlain, J. Morgerman, L. K. Shay and C. Velden (2017) Re-writing the tropical record books: The extraordinary intensification of Hurricane Patricia (2015), Bulletin of the American Meteorological Society, doi: 10.1175/BAMS-D-16-0039.1.

Usui, N., S. Ishizaki, Y. Fujii, H. Tsujino, T. Yasuda and M. Kamachi (2006). Meteorological Research Institute multivariate ocean variational estimation (MOVE) system: Some early results. Advances in Space Research, 37(4), 806-822.

Wada, A., N. Kohno and Y. Kawai (2010). Impact of wave-ocean interaction on Typhoon Hai-Tang in 2005. SOLA, 6A, 13-16.